




A WDM Network Controller With Real-Time Updates of the Physical Layer Abstraction

Tianliang Zhang , Azadeh Samadian, Ali Shakeri, Behzad Mirkhanzadeh, Chencheng Shao, Miguel Razo, Marco Tacca, Alessio Ferrari , Mattia Cantono, Vittorio Curri, *Senior Member, IEEE*, Giovanni Martinelli, Gabriele Maria Galimberti , Tiejun Xia, Glenn Wellbrock, and Andrea Fumagalli

Abstract—This paper describes the implementation of a wavelength division multiplexing network controller that accounts for the varying conditions of the network physical layer in real time. A newly added software module is used to estimate the physical layer quality of transmission (QoT-E) in the form of a single transmission figure of merit for every line span in the network, i.e., the optical signal-to-noise ratio (OSNR) degradation. The estimated OSNR degradation is used to verify lightpath feasibility in the network, and produce optimal routing and wavelength assignment solutions in real time, without the need for a separate network planning tool. The OSNR degradation is estimated without requiring detailed knowledge of the optical components deployed in the network, and consequently the approach is vendor agnostic. The accuracy of the estimated OSNR degradation is assessed experimentally, and its impact on two network-wide performance indicators is studied through simulation.

Index Terms—Quality of transmission, real-time estimation, signal power margin, software defined networking, wavelength division multiplexing.

I. INTRODUCTION

WDM networks have been traditionally designed to provide fixed virtual network connectivity to the packet-switched electronic upper layers (e.g., Ethernet, IP) in the form of static lightpaths that interconnect pairs of switches or routers.

Manuscript received December 15, 2018; revised June 3, 2019; accepted June 13, 2019. Date of publication June 21, 2019; date of current version July 31, 2019. This work was supported by National Science Foundation under Grants CNS-1405405, CNS-1409849, ACI-1541461, and CNS-1531039. (*Corresponding author: Tianliang Zhang.*)

T. Zhang, A. Samadian, A. Shakeri, B. Mirkhanzadeh, M. Razo, M. Tacca, and A. Fumagalli are with the University of Texas at Dallas, Richardson, TX 75080 USA (e-mail: txz160730@utdallas.edu; Azadeh@utdallas.edu; alishakeri@utdallas.edu; behzad@utdallas.edu; mrazo@utdallas.edu; mtacca@utdallas.edu; andrea@utdallas.edu).

C. Shao was with the University of Texas at Dallas, Richardson, TX 75080 USA. He is now with Comtech TeleCommunications, Seattle, WA 98121 USA (e-mail: chenchengshao@gmail.com).

A. Ferrari and V. Curri are with the Polytechnic University of Turin, 10129 Torino, Italy (e-mail: alessio.ferrari@polito.it; vittorio.curri@polito.it).

M. Cantono was with the Polytechnic University of Turin, 10129 Torino, Italy. He is now with Google Inc., Mountain View, CA 94043 USA (e-mail: mattiacantono@gmail.com).

G. Martinelli and G. M. Galimberti are with Cisco Photonic, 20871 Vimercate, Italy (e-mail: giomarti@cisco.com; ggalimbe@cisco.com).

T. Xia and G. Wellbrock are with Verizon, Dallas, TX 75224 USA (e-mail: tj.xia@verizon.com; glenn.wellbrock@verizon.com).

Color versions of one or more of the figures in this paper are available online at <http://ieeexplore.ieee.org>.

Digital Object Identifier 10.1109/JLT.2019.2924397

To account for the various transmission constraints that originate at the optical physical layer [1], the static virtual network is usually designed manually with the assistance of a network planning tool, which verifies each lightpath feasibility based on the anticipated network fiber layout and optical equipment that will be deployed. The planning tool output is then used to configure the network equipment, which in turn establishes the lightpaths as computed by the tool. During this process, the planning tool is programmed to account for end-of-life transmission merit figures of the optical fibers and equipment, and other uncertainties [2] — a procedure that typically requires significant power budget margins to be applied to the feasible lightpaths. This approach is conservative and well established, but is known to cause network resource under-utilization [3], as also documented in Section V-B of this paper.

Solutions that provide information about the lightpath power budget margin in real-time are based on either legacy intensity-modulation direct-detection (IMDD) transmission systems [4] or vendor specific and proprietary technologies [5], [6]. A summary of these and other related solutions is provided in Section II.

This paper describes the implementation of a vendor-agnostic network controller that in real-time accounts for the physical layer varying conditions of WDM networks, which operate with modern, uncompensated, multilevel modulation, commercial products. The network controller makes use of a newly added QoT-E software module to estimate the physical layer quality of transmission in the form of a single transmission figure of merit for every line span in the network, i.e., the OSNR degradation. The QoT-E module is invoked to process transmission line parameters that are periodically extracted from the network equipment and provides real-time line span OSNR degradation estimates using fast and accurate modeling techniques [7], [8]. These estimates are then used by the controller path computation engine to verify feasibility of lightpaths (either established or yet to be established) in the network, and produce optimal routing and wavelength assignment (RWA) solutions that account for such real-time lightpath feasibility constraints.

The described implementation has the following advantages. Lightpath feasibility can be verified by the network controller in real-time without the need for a separate network planning tool manually operated. As discussed in Section V-A, the accuracy of the OSNR degradation estimated by the QoT-E module may be as good as 1 dB, which in turn enables the network

controller to relay on reduced power margins when assessing lightpath feasibility. When applicable, small power margins may lead to lightpath routing solutions that yield improved network capacity and reduced optical transponder count as discussed in Section V-B. In addition, the OSNR degradation is estimated without requiring detailed knowledge of the optical components deployed in the network. Consequently, the approach is vendor independent and applicable to any WDM network.

II. PRIOR WORK

Software Defined Networking (SDN) controllers are used in transport networks to discover and manage network resources effectively across multiple layers (physical, OTN, Ethernet). A number of SDN demonstrations has been reported as part of the Open Networking Foundation (ONF) [9]. In [9], most demonstrations concentrate on higher layers in the networking stack, and only two demonstrations mention control of multi-vendor optical layer. The first is driven by Sedona Systems [10] and displays an orchestrator interfacing with each vendor proprietary SDN controller. The second is driven by ONOS [11]. According to [9], the demo consisted of an emulation of a live environment with the expectation of soon achieving a demo in a production environment. Another recent demonstrator is reported by Sendate [12], conducted in the Telia Company R&D lab in Stockholm [13], with live connectivity to production network fibers, multi-vendor and multi-domain field trials, and with physical impairments being handled through the VPIphotonics Design Suite [14]. There are also proprietary solutions offered by vendors, like [5], [6]. Detailed information about the procedures followed to account for the optical transmission impairments is not provided for these demonstrations and proprietary solutions.

There is a rich literature on SDN solutions for optical networks [4], [15]–[20]. These solutions account for lightpath provisioning, wavelength continuity, flex grid spectrum assignment [19], Application-Based Network Operation (ABNO) architecture [20], optical performance monitoring and congestion-aware routing [17], multi-layer interdependence [18], data center rack-to-rack connectivity over optical network [15], and support for radio access networks [16]. All but [4] do not account for optical transmission impairments in real-time, nor pursue vendor-agnostic solutions.

The solution in [4] interfaces a path computation element (PCE) — equipped with physical impairment-aware routing capabilities — with a network management system (NMS). The two modules are tightly synchronized, with the PCE module able to provide feasible routes for the optical circuits to be created by NMS through GMPLS, which is the chosen control plane for the optical network. The physical impairment model implemented in PCE [21] accounts for legacy RZ modulation, dispersion-managed line span, and polarization mode dispersion (PMD), which is an important factor in legacy IMDD modulations.

Concerning recent transmission technologies based on coherent and multilevel modulation formats, machine learning techniques have been proposed to deal with physical impairment [22], [23]. In [22] a vendor-agnostic (open ROADM) SDN controller makes use of a path quality estimator module that is

used to estimate the bit error rate (BER) of a requested lightpath service before its creation. Through a learning process, the path quality estimator module improves the accuracy of the estimated BER achieving over time an error margin of 1.2 dB. In [23], machine learning techniques are applied to metrics that are obtained from the line card to predict QoT based on data obtained from a network-wide monitoring database. To train the machine learning models, these solutions require extensive data collection from the optical network and are not suitable for greenfield deployment.

In long-haul WDM networks, the optical path quality is mostly affected by the amplified spontaneous emission (ASE) noise — introduced by amplifiers — and nonlinear interference (NLI) — introduced by the optical fiber. The work in [24] evaluates the NLI using a cross phase modulation (XPM) model. Such a model is based on legacy communication systems. Another approach to estimate the NLI makes use of the Gaussian noise (GN) model [25], which has been developed to account for optical coherent communications technologies. Optical fiber is a non-linear propagation medium that distorts the signal. The GN model offers an abstraction of a fiber span to consist of a linear medium plus an additive white Gaussian noise (AWGN) source, which accounts for the NLI. Thus, it is possible to abstract a line span (LS) as a linear block plus an overall AWGN source, whose power is the sum of ASE noise power (P_{ASE}) and NLI noise power (P_{NLI}). In such a way, the optical performance of a LS is uniquely identified by a single figure of merit, i.e.,

$$OSNR_{LS} = \frac{P_S}{P_{ASE} + P_{NLI}}, \quad (1)$$

where P_S is the signal power. As shown in [8], the classic GN model can be used to estimate P_{NLI} for narrow bands up to 3 THz of occupied band. However, for wider bands, the Raman crosstalk is no longer negligible. For this reason a generalized GN model is proposed in [26]–[28] and validated in [29]–[31]. In the absence of detailed information about the fiber spectral utilization a conservative and reasonable approach is to assume a full spectral load when estimating the $OSNR_{LS}$ [32].

III. QOT ESTIMATION MODULE

The QoT-E module is implemented to assist the SDN controller in estimating the path OSNR at the receiver. The estimation may be performed without having to first commission the optical circuit along the path. To do so, the module makes use of specific input parameters and a series of equations (collectively referred to as Gaussian noise or GN model), described in this section.

The first step is to estimate the OSNR degradation of each LS in the network, defined as the transmission line (inclusive of booster, line, and pre-amplifier) between two connected ROADM nodes. (Note that the booster gain is set to compensate for the signal attenuation incurred inside the ROADM.) The span OSNR is evaluated as (1). The P_{ASE} for each amplifier in the LS is estimated by [4]

$$P_{ASE} = hf_0FB_{ref}(G - 1), \quad (2)$$

where h is the Plank constant, f_0 is the central frequency of the C-band, F is the amplifier noise figure, B_{ref} is the resolution bandwidth (RBW) of the OSNR measurement, and G is the amplifier gain. P_{NLI} is evaluated using the GN model [25]

$$P_{NLI} = P_S^3 \frac{16}{27\pi} \frac{\alpha}{|\beta_2|} \gamma^2 \frac{L_{eff}^2}{R_s^2} \ln \left(\frac{\pi^2}{2} |\beta_2| \frac{R_s^2}{\alpha} \left(\frac{B_{opt}}{\Delta f} \right)^{2 \frac{R_s}{\Delta f}} \right), \quad (3)$$

where α is the fiber attenuation, β_2 is the chromatic dispersion coefficient, γ is the nonlinear coefficient, L_{eff} is the effective fiber length, R_s is the symbol rate, B_{opt} is the occupied bandwidth and Δf is the frequency offset. The values of these input parameters must be provided to the QoT-E module, and for those parameters that may be subject to changes, real-time refreshes are extracted from the equipment as described in Section IV. In particular, the fiber attenuation coefficient, the chromatic dispersion coefficient, and the nonlinear coefficient are all assumed to be time-invariant and provided through a flat file. The amplifier gain is directly obtained from the equipment. The amplifier noise figure is extracted from the product datasheet and provided through a flat file. The length of the fiber connecting two adjacent amplifiers is indirectly computed from the fiber attenuation coefficient and the power level difference between the output of the upstream amplifier and the input of the downstream amplifier. While this is not a highly accurate approach to estimating the fiber length, it suffices to provide a reasonable estimate of this input parameter for the computation of P_{NLI} .

Once the OSNR value for every line span of the network is estimated as in (1), the SDN controller can update the network abstraction with a single figure of merit that summarizes the physical characteristics of the fiber medium. Thus, the network fiber topology can be represented by a weighted direct graph where each arc, representing a specific line span, is assigned the weight of $OSNR_{LS}^{-1}$. Using this graph, the SDN controller is able to estimate the connection path OSNR by simply adding the weights of the arcs in the path [4]:

$$OSNR_{Path} = \left(\sum_{LS,i} \frac{1}{OSNR_{LS,i}} \right)^{-1}. \quad (4)$$

The estimate in (4) assumes that noise power accumulates independently at each network element in the connection path, and it is therefore estimated by summing the noise power each element contributes to the connection path normalized to the signal power.

While the real-time extraction of the input parameter values from the equipment may require a vendor-dependent procedure, the QoT-E module makes use of a computation that is vendor-agnostic. So long as the required input parameter values are accurately collected from the network equipment, this approach can estimate the path OSNR without requiring detailed knowledge of the optical components deployed in the network, e.g., the ROADM node specific architecture. The GN model ((1)–(4)) in its closed form solution can expeditiously compute the P_{NLI} component, thus providing updates of the span and path OSNR values in real-time. Leveraging these real-time values the SDN

controller can predict the bitrate feasibility of any path even before the optical circuit is commissioned along that path. This can be performed by just verifying whether the path OSNR predicted through the output provided by the QoT-E module is above or below the receiver OSNR minimum threshold for that chosen bitrate and modulation format. By knowing the bitrate feasibility of a given path, the SDN controller can use the maximum allowed bitrate for each connection (service) request, subject to the availability of suitable optical transponders.

IV. UPGRADING THE PRONET SDN ORCHESTRATOR WITH THE GN-BASED QoT-E MODULE

The GN-based QoT-E module was recently implemented in C++ and integrated with the SDN Orchestrator¹ of the PRONet (Programmable Optical network) test-bed [33]. PRONet is a two-layer Research and Education Network (REN) under development and deployment at and around the UT Dallas campus. The PRONet Orchestrator provides three critical functions in an Ethernet-over-WDM network. First, the Orchestrator discovers the whole two-layer network and creates a multi-layer graph representation of the same. For each packet flow request, it computes two shared risk link group (SRLG) disjoint paths against its graph: one as primary and the other as secondary. Second, the Orchestrator provisions any required lightpaths and pushes the OpenFlow rules to the SDN enabled packet switches. Third, it performs protection and restoration mechanisms in times of failure. The protection mechanism is handled by the packet switch data plane. The switches that are connected to the failed link redirect the traffic from the primary to the secondary path using the pre-installed OpenFlow rules featuring fast failover groupable functionality. The restoration mechanism is activated by the Orchestrator, which sends a request to the optical domain controller to establish a lightpath that replaces the disrupted original primary path.

As shown in Fig. 1, the PRONet Orchestrator makes use of a database which serves as a network inventory and information exchanger between a few key modules. The Resource Management (RM) module is the orchestrator interface to the optical and packet domain. It discovers packet network topology and pushes the node configuration using REST APIs provided by one of the three open-source packet domain controllers (OpenDaylight, Floodlight or Ryu). It also interacts with optical nodes through a vendor-specific RESTCONF optical plugin (Cisco in the experiment presented in this paper) to fill out the database and create or delete lightpaths. The RESTCONF optical plugin provides a programmatic interface for accessing data defined in YANG, using the datastores defined in NETCONF. Path computation is performed by the Service Provisioning (SP) module, which applies various shortest path algorithms to the graph abstraction of the network. Finally, the SP module sends the service creation request to the RM module to issue the lightpath creation and packet switch configurations.

With the inclusion of the GN-based QoT-E module, the PRONet Orchestrator can now estimate with a given accuracy

¹The term SDN Orchestrator is used to reflect the multi-layer nature of this SDN controller.

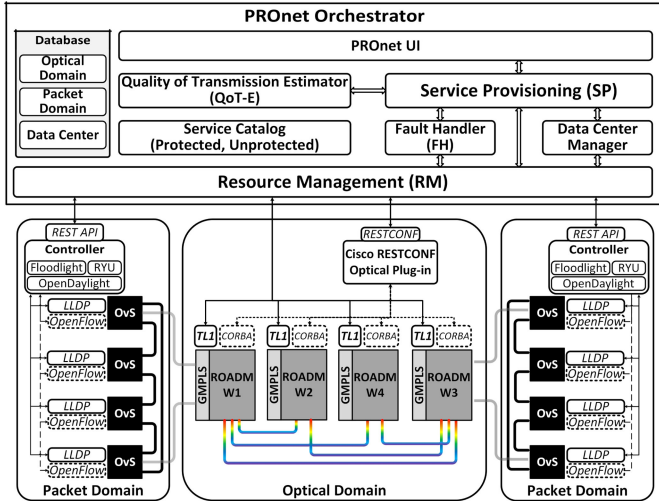


Fig. 1. Architecture of the PRONet SDN orchestrator.

the path OSNR in real-time. Before provisioning a lightpath the SP module can invoke the assistance of the QoT-E module in order to estimate the feasibility of any chosen lightpath. For every lightpath of interest the SP module computes the estimated path OSNR using (4) and verifies whether it exceeds the receiver minimum required OSNR threshold. Lightpaths that satisfy this requirement are classified as ‘feasible’. The SP module then provisions the lightpath request after selecting one of the feasible paths based on a desired objective function, e.g., shortest propagation delay, least congested path, highest signal power budget margin. With this functionality the PRONet Orchestrator is able to offer more routing strategies, besides the conventional minimum hop-count, without requiring the assistance of a manually operated network planning tool to ensure the feasibility of the lightpath.

The Orchestrator database is used to store and periodically update the transmission parameters that are required by the QoT-E module. These parameters, including network channel spacing and symbol rate, modulation format, fiber attenuation, and total number of channels are discovered through the optical RESTCONF plugin. Additional parameters that are not available through the RESTCONF plugin are discovered through the Transaction Language 1 (TL1) protocol. The Orchestrator is directly connected to the WDM network elements and uses a TL1 plugin in the RM module to periodically send TL1 commands to the ROADM nodes and line amplifiers. Critical optical line span parameters are periodically extracted from the equipment and stored in the database, including booster amplifier gain, pre-amplifier gain, power per channel at both the booster amplifier input and pre-amplifier output. During this periodic procedure the RM module also compares the reference values (as pre-defined by the network planning tool) against the actual values (when at least one circuit is provisioned) in order to promptly detect anomalies in the physical layer. Other relevant (but considered fixed) parameters such as fiber attenuation coefficient, chromatic dispersion coefficient, nonlinearity coefficient, noise figure, insertion loss, and OSNR receiver threshold are provided through a flat file and stored in the database at the Orchestrator

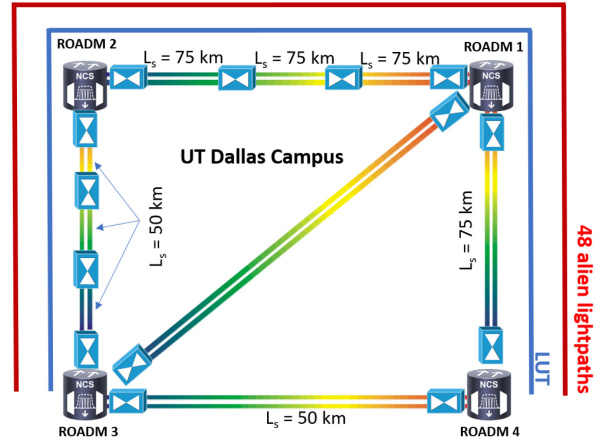


Fig. 2. PRONet topology.

start time. With these parameters (some of which are updated in real-time) available in the database, the invoked QoT-E module can compute each line span OSNR degradation in real-time.

V. RESULTS

A. QoT-E Module Validation Experiment

Validation of the QoT-E implementation is experimentally performed using the PRONet test-bed, whose optical layer is shown in Fig. 2. Four Cisco NCS2K CDC ROADMs are deployed and make use of one SMR9 Cisco module on each degree.

Each SMR9 has a booster amplifier (outgoing signal) and a pre-amplifier (incoming signal). The ROADM 1-ROADM 2 line span is equipped with two Cisco EDFA24 line amplifiers in tandem with 75 km of standard single mode fiber (SSMF). The ROADM 2-ROADM 3 line span is equipped with two Cisco EDFA17 line amplifiers in tandem with 50 km of SSMF. The ROADMs are configured to operate in 50 GHz ITU fixed grid.

The Path OSNR estimated by the QoT-E module is compared against the actual OSNR of an established lightpath, referred to as lightpath under test (LUT). The LUT carries a PM-16QAM root-raised cosine (RRC) signal with central wavelength 1547.32 nm. Its symbol rate is 32 GBaud and the signal carries 200 Gbps. As shown in Fig. 2, the LUT originates at ROADM 4 and ends at ROADM 3, passing through ROADM 1 and ROADM 2. The LUT path is 450 km long and transparently passes through 2 ROADM nodes and 10 erbium-doped fiber amplifiers (EDFAs).² Each booster amplifier gain is set to recover the attenuation inside the ROADM and to reach the target signal power level of the outgoing line span. The line span target power level is chosen to maximize the line span OSNR in (1), which can be shown to also maximize the OSNR of the connection path in (4). This strategy is referred to as local-optimization global-optimization or LOGO [34].

In order to have a realistic spectral load, and thus a realistic NLI effect in the experiment, 48 alien lightpaths are generated

²Of the 10 EDFAs, 3 are booster amplifiers, 3 are pre-amplifiers and 4 are line amplifiers.

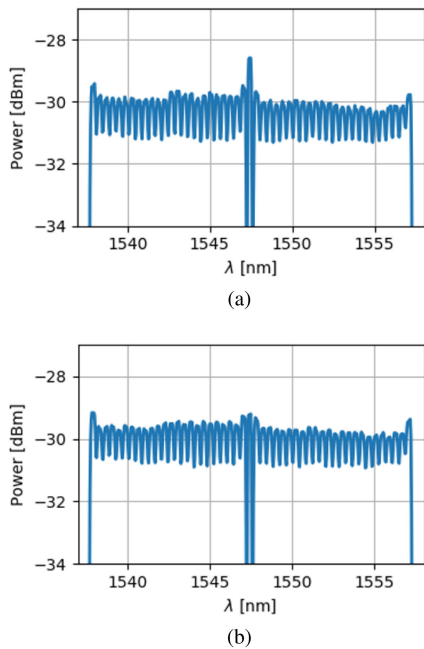


Fig. 3. Pre-booster signal comb using (a) flat power across WDM channels and (b) flat power spectral density (PSD). The resolution bandwidth is 0.06 nm.

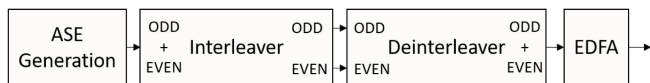


Fig. 4. Block diagram of system used to generate 48 alien channels.

in the 50 GHz fix grid with the LUT being placed in the middle of the comb, as shown in Fig. 3a and 3b. The alien lightpaths are generated using the setup depicted in Fig. 4. The setup consists of an ASE noise generator — an EDFA with no input signal — properly filtered using an interleaver. In such a way an ODD comb and an EVEN comb are generated. The resulting spectra have a -3 dB bandwidth of 37.5 GHz. Subsequently, the two combs are combined together using a deinterleaver. Before being launched into the network the combined combs are amplified using an EDFA in order to satisfy the minimum power level that is required by the Cisco ROADMs to properly detect their presence as alien lightpaths. The 48 alien lightpaths are then routed through the network along with the LUT.

Two channel power distribution scenarios are tested. In the first scenario (a), a flat power per channel is used, i.e., each WDM channel signal power is set to be equal to a nominal value (Fig. 3a). In the second scenario (b), in order to have a condition close to the Nyquist WDM, a flat power spectral density (PSD) is used, i.e., the LUT is attenuated by 0.7 dB to keep its peak power closer to the peak power of the alien channels (Fig. 3b). The nominal (zero offset) transmitted power set at the booster amplifiers is computed according to the LOGO strategy. For each scenario, a power sweep is also performed, i.e., the transmitted power is varied within a small interval around this nominal LOGO-based value. The power sweep is achieved across the entire WDM comb by varying the booster gain and output power accordingly. The power offset ranges from -1 dB

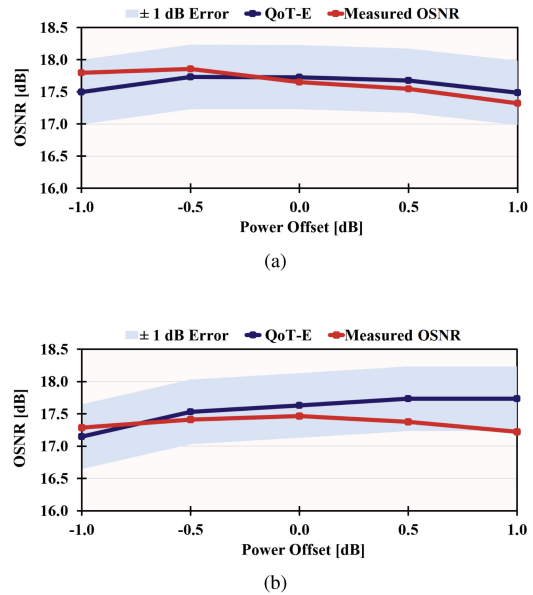


Fig. 5. Comparison of LUT path OSNR as predicted by the QoT-E module (square) and measured experimentally (circle) in the presence of (a) flat power per channel and (b) flat PSD. The light blue shaded bands represent the ± 1 dB error range.

to $+1$ dB with steps of 0.5 dB. For each scenario and for each value of the power offset, the pre-forward error correction (FEC) BER is recorded from the line card. The average BER is computed over 15 minute intervals. The experimental path OSNR is then indirectly computed from the average BER using the transponder back-to-back curve. The resolution bandwidth applied to measure the OSNR is set to the signal symbol rate, i.e., 32 GHz. Concurrently, the path OSNR for each experiment is also predicted using the QoT-E module. The results are reported in Fig. 5. The curves with square markers report the prediction provided by QoT-E module, while the curve with circle markers reports the actual LUT OSNR. The light blue shaded bands represent the ± 1 dB range of uncertainty of the QoT-E prediction. In all of our experiments the QoT-E prediction is within ± 1 dB of the actual LUT OSNR value, corroborating earlier results based on the same computation procedure implemented in the QoT-E module [8]. It can also be noted that the actual OSNR is sometime lower than the predicted one, suggesting that the typical conservative estimation of the GN model, here, does not hold. This anomaly is due to the system parameters' uncertainty (observational errors) which erodes away such conservative margin. Furthermore, at the optimum power (zero offset) the maxima predicted by the QoT-E module are quite close to the reported experimental values, with an error that is lower than 1 dB. The next section investigates the effect of introducing a signal power margin to account for the error introduced by the QoT-E computed path OSNR.

B. Network Wide Simulation Results

As discussed in the previous section, the path OSNR estimate provided by the QoT-E module is within 1 dB from the actual value in our experiment. Conservatively, a power margin

must be added by the Orchestrator to compensate for this error. Having to apply a power margin on the QoT-E estimated path OSNR is likely to introduce network performance degradation and/or increased cost. Network-wide simulation results are presented in this section to assess two performance indicators, i.e., the achievable throughput in the network subject to a pre-defined target tablocking probability, and the average number of optical transponder pairs that must be deployed for each accepted lightpath request.

Using a network-wide simulation allows us to test with a number of fiber topologies and varying number of optical nodes. Three network topologies are considered, i.e., the Japanese graph [35], the COST 239 [36] and the Spanish. For each fiber span of these three networks the simulation is conducted using the following assumptions. It is assumed that the fiber attenuation coefficient is 0.22 dB/km, the reference wavelength is 1545 nm, chromatic dispersion coefficient is 16.7 ps/nm/km, and the nonlinear coefficient is 0.0013 1/W/m. A 0.5 nm resolution bandwidth is used when referring to OSNR values. Other relevant parameters for the calculation of the line span OSNR and their values are as in [37]. Four power margins are applied to the path OSNR estimated using (4), i.e., 0, 1, 2, and 3 dB. These margin values increasingly reduce the power budget available in every path and are representative of growing uncertainty in the QoT-E provided OSNR estimates. Incoming service requests are in the form of 200 Gbps end-to-end circuits between node pairs randomly chosen in the graph. Incoming service requests form a Poisson process and each admitted service has a random holding time with exponential distribution. A service request can be fulfilled using either a single pair of PM-16QAM (200G) transponders, or two pairs of PM-QPSK (100G) transponders. The former solution requires 50 GHz of spectrum slice, and a path OSNR that must be at least 13.8 dB. The latter solution requires two (non-contiguous) spectrum slices of 50 GHz each, which are assigned the same path with OSNR that is at least 5.1 dB. When applicable, the former solution is preferred as it requires only one spectrum slice and one pair of transponders. An incoming service request is blocked when both solutions cannot be applied, e.g., spectrum slices (80 spectrum slices are simulated in each fiber span) are not available on any of the computed paths (5 shortest paths are pre-computed for every node pair with increasing path inverse OSNR value).

Fig. 6 shows the network blocking probability versus offered load (in Erlang) while varying the applied power margin in the Japanese network. The offered load is defined as the product between service request arrival rate and average holding time. The achievable throughput, defined as the offered load that causes a pre-determined target blocking probability of 10^{-5} , is summarized for the Japanese, Cost 239, and Spanish topology in Table I. For all three topologies the achievable throughput decreases monotonically as the applied margin is changed from 0 to 3 dB. The throughput reduction varies from topology to topology as it is determined by the specific distribution of the path lengths in each topology. The same table also shows in parenthesis the time-average number of transponder pairs deployed per service request. In both the Japanese and Spanish topology this value is close to 1 when the 0 dB margin is applied, indicating that almost all of the service requests can be fulfilled with a single

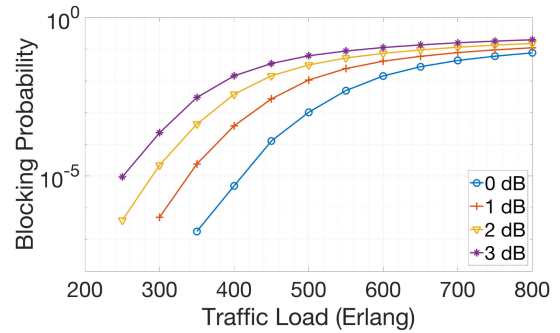


Fig. 6. Blocking probability versus traffic offered load (in Erlang) for the Japanese topology with varying applied power margin.

TABLE I
ACHIEVABLE THROUGHPUT AND AVERAGE NUMBER OF PER-SERVICE
TRANSPONDER PAIRS FOR DIFFERENT TOPOLOGIES AND DIFFERENT OSNR
POWER MARGINS

Topology	Different power margin			
	0 dB	1 dB	2 dB	3 dB
COST 239	450 (1.61)	430 (1.71)	400 (1.80)	380 (1.84)
Japanese	420 (1.08)	350 (1.16)	300 (1.28)	250 (1.43)
Spanish	560 (1.06)	460 (1.15)	350 (1.47)	340 (1.49)

200 Gbps transponder pair. However, when non-zero margin values are applied, this average increases to almost 1.5, indicating that half of the established services require two transponder pairs, each operating at 100 Gbps. For the Cost 239 topology the average number of transponder pairs is higher compared to the other two topologies due to its larger geographical footprint.

Both the experimental results in Section V-A and the simulation results in this section are obtained assuming that line spans are spectrally fully loaded. This assumption represents the worst possible NLI scenario and can be seen as a conservative estimate that is valid under any load distribution. This conservative estimate may be relaxed in the presence of light load distributions. When the line span spectrum is lightly loaded the resulting P_{NLI} in (3) is reduced, and both $OSNR_{LS}$ in (1) and $OSNR_{Path}$ in (4) are improved. Studies have shown that OSNR-driven spectrum assignment constraints can improve the average path OSNR by limiting the permitted load distribution of the line span spectrum while at the same time only marginally impacting the network blocking probability [38].

VI. CONCLUSION

In this paper the PRoNet SDN Orchestrator is upgraded with a newly designed QoT-E module, which provides real-time updates of a single transmission figure of merit applied to every line span and lightpath in a WDM network. The figure of merit is the line span OSNR degradation that is first computed by the QoT-E module analytically from a number of input parameters that are periodically extracted from the equipment by the Orchestrator. In turn, the Orchestrator compares the path OSNR (computed from the line span OSNR) against the receiver OSNR minimum threshold for each specific bitrate and modulation format of interest. Through this comparison, the Orchestrator can predict the

feasibility of any given path in the network even before establishing the actual optical circuit along that path. Through this procedure, the Orchestrator can optimally compute and select feasible paths in the WDM network while accounting for its physical impairments in real-time. While the input parameter value extraction from the equipment may be vendor dependent, the analytical computation of the path OSNR is vendor-agnostic, and does not need to account for the specific architecture of the used equipment, e.g., optical components in the ROADM. A drawback of the implemented solution is the uncertainty (observational error) of the measured input parameter values, which propagates to the computed path OSNR value. Experimentally, observational error was found to nullify the typical conservative estimation produced by the analytical model implemented in the QoT-E module. For this reason, a power margin must be applied to the computed path OSNR, e.g., 1 dB. The effect of the applied power margin value on the network performance and efficiency is studied through simulation, revealing that the use of high margin values may cause a loss of network achievable throughput as high as 40%, and an increase in required optical transponder pairs as high as 50%. Improving the accuracy of the path OSNR estimated by the QoT-E module would permit the Orchestrator to reduce the applied power margin value and improve both network performance and efficiency.

REFERENCES

- [1] M. Cvijetic *et al.*, *Advanced Optical Communication Systems and Networks*. Norwood, MA, USA: Artech House, 2013.
- [2] I. Kaminow *et al.*, *Optical Fiber Telecommunications VB: Systems and Networks*. Amsterdam, The Netherlands: Elsevier, 2010.
- [3] Y. Pointurier, "Design of low-margin optical networks," in *Proc. Opt. Fiber Commun. Conf. Exhib.*, Mar. 2016, pp. 1–3.
- [4] T. Tsuritani *et al.*, "Optical path computation element interworking with network management system for transparent mesh networks," in *Proc. Conf. Opt. Fiber Commun./Nat. Fiber Opt. Eng. Conf.*, Feb. 2008, pp. 1–10.
- [5] "Infinera: A software defined network architecture for transport networks," 2015. [Online]. Available: <https://www.infinera.com/pdfs-cpt/a-software-defined-network-architecture-for-transport-networks/>
- [6] "Ciena blueplanet: Intelligent automation driving digital transformation for service providers," 2019. [Online]. Available: https://media.ciena.com/documents/Intelligent_Automation_WP.pdf
- [7] M. Cantono *et al.*, "Observing the interaction of PMD with generation of NLI in uncompensated amplified optical links," in *Proc. Opt. Fiber Commun. Conf. Expo.*, Mar. 2018, pp. 1–3.
- [8] M. Filer *et al.*, "Multi-vendor experimental validation of an open source QoT estimator for optical networks," *J. Lightw. Technol.*, vol. 36, no. 15, pp. 3073–3082, Aug. 1, 2018.
- [9] "ONF: The SDN solutions showcase technical report and analysis. 2015. [Online]. Available: https://www.opennetworking.org/images/stories/downloads/sdn-resources/white-papers/ONF_SDN%20Solutions%20Showcase%20WhitePaper_2015.pdf
- [10] Sedona systems, 2019. [Online]. Available: <https://sedonasys.com/>
- [11] Onos, 2019. [Online]. Available: <https://onosproject.org/>
- [12] "Celtic-plus project sendate simplifies operations of open optical networks," 2018. [Online]. Available: <https://www.celticnext.eu/celtic-plus-project-sendate-simplifies-operations-of-open-optical-networks/>
- [13] Telia company, 2019. [Online]. Available: <https://www.teliacompany.com/en>
- [14] Vpiphotonics, 2019. [Online]. Available: <https://www.vpiphotonics.com/>
- [15] P. Samadi *et al.*, "Experimental demonstration of converged inter/intra data center network architecture," in *Proc. 17th Int. Conf. Transparent Opt. Netw.*, Jul. 2015, pp. 1–4.
- [16] M. Fiorani *et al.*, "Transport abstraction models for an SDN-controlled centralized ran," *IEEE Commun. Lett.*, vol. 19, no. 8, pp. 1406–1409, Aug. 2015.
- [17] J. M. Fábrega *et al.*, "Demonstration of adaptive SDN orchestration: A real-time congestion-aware services provisioning over OFDM-based 400g OPS and flexi-WDM OCS," *J. Lightw. Technol.*, vol. 35, no. 3, pp. 506–512, Feb. 1, 2017.
- [18] F. Paolucci *et al.*, "Open network database for application-based control in multilayer networks," *J. Lightw. Technol.*, vol. 35, no. 9, pp. 1469–1476, May 1, 2017.
- [19] R. Morro *et al.*, "Automated end to end carrier ethernet provisioning over a disaggregated WDM metro network with a hierarchical SDN control and monitoring platform," in *Proc. Eur. Conf. Opt. Commun.*, Sep. 2018, pp. 1–3.
- [20] V. López, *et al.*, "Control plane architectures for elastic optical networks," *J. Opt. Commun. Netw.*, vol. 10, no. 2, pp. A241–A249, Feb. 2018.
- [21] J. Antona *et al.*, "Nonlinear cumulated phase as a criterion to assess performance of terrestrial WDM systems," in *Proc. Opt. Fiber Commun. Conf. Exhibit*, Mar. 2002, pp. 365–367.
- [22] S. Oda *et al.*, "A learning living network with open ROADMs," *J. Lightw. Technol.*, vol. 35, no. 8, pp. 1350–1356, Apr. 15, 2017.
- [23] S. Yan *et al.*, "Field trial of machine-learning-assisted and SDN-based optical network planning with network-scale monitoring database," in *Proc. Eur. Conf. Opt. Commun.*, Sep. 2017, pp. 1–3.
- [24] F. Cavaliere *et al.*, "Modeling and distributed provisioning in 10–40–100-Gb/s multirate wavelength switched optical networks," *J. Lightw. Technol.*, vol. 29, no. 9, pp. 1248–1257, May 1, 2011.
- [25] P. Poggiolini *et al.*, "The GN-model of fiber non-linear propagation and its applications," *J. Lightw. Technol.*, vol. 32, no. 4, pp. 694–721, Feb. 15, 2014.
- [26] M. Cantono *et al.*, "Introducing the generalized GN-model for nonlinear interference generation including space/frequency variations of loss/gain," 2017, arXiv:1710.02225.
- [27] I. Roberts *et al.*, "Channel power optimization of WDM systems following gaussian noise nonlinearity model in presence of stimulated raman scattering," *J. Lightw. Technol.*, vol. 35, no. 23, pp. 5237–5249, Dec. 1, 2017.
- [28] D. Semrau *et al.*, "The gaussian noise model in the presence of inter-channel stimulated raman scattering," *J. Lightw. Technol.*, vol. 36, no. 14, pp. 3046–3055, Jul. 15, 2018.
- [29] M. Cantono *et al.*, "Modelling the impact of SRS on NLI generation in commercial equipment: An experimental investigation," in *Proc. Opt. Fiber Commun. Conf. Expo.*, Mar. 2018, pp. 1–3.
- [30] M. Cantono *et al.*, "On the interplay of nonlinear interference generation with stimulated raman scattering for QoT estimation," *J. Lightw. Technol.*, vol. 36, no. 15, pp. 3131–3141, Aug. 2018.
- [31] M. Cantono *et al.*, "Physical layer performance of multi-band optical line systems using raman amplification," *J. Opt. Commun. Netw.*, vol. 11, no. 1, pp. A103–A110, Jan. 2019.
- [32] V. Curri *et al.*, "Design strategies and merit of system parameters for uniform uncompensated links supporting Nyquist-WDM transmission," *J. Lightw. Technol.*, vol. 33, no. 18, pp. 3921–3932, Sep. 15, 2015.
- [33] B. Mirkhanzadeh *et al.*, "An SDN-enabled multi-layer protection and restoration mechanism," *Opt. Switching Netw.*, vol. 30, pp. 23–32, 2018.
- [34] P. Poggiolini *et al.*, "The logon strategy for low-complexity control plane implementation in new-generation flexible networks," in *Proc. Opt. Fiber Commun. Conf. Expo. Nat. Fiber Opt. Eng. Conf.*, Mar. 2013, pp. 1–3.
- [35] R. Casellas *et al.*, "SDN orchestration of openflow and gmpls flexi-grid networks with a stateful hierarchical PCE [invited]," *IEEE J. Opt. Commun. Netw.*, vol. 7, no. 1, pp. A106–A117, Jan. 2015.
- [36] A. Morea *et al.*, "Protocol enhancements for "greening" optical networks," *Bell Labs Tech. J.*, vol. 18, no. 3, pp. 211–230, Dec. 2013.
- [37] Y. Fei, "Impacts of physical layer impairments on optical network performance," Ph.D. dissertation, Erik Jonsson Sch. Eng. Comput. Sci., Univ. Texas Dallas, Richardson, TX, USA, 2017.
- [38] Y. Fei *et al.*, "Spectrum assignment constraints for improved OSNR in optical networks with dynamic traffic," in *Proc. IEEE 18th Int. Conf. High Perform. Switching Routing*, Jun. 2017, pp. 1–6.

Tianliang Zhang was born in Nanjing, China in 1994. He received the B.S. degree in optoelectronic information engineering from the Nanjing University of Science and Technology, Nanjing, China, in 2016. He is currently working toward the M.S. and Ph.D. degrees in electrical engineering with the University of Texas at Dallas, Richardson, TX, USA. His research interests are optical networks modeling and optical communication system impairment analysis.

Azadeh Samadian received the M.S. degree in electrical engineering from Shahid Beheshti University, Tehran, Iran, in 2014. She is currently working toward the Ph.D. degree with the University of Texas at Dallas, Richardson, TX, USA. Her research interests are network planning, resource efficiency, and performance evaluation in optical networks.

Ali Shakeri received the B.S. degree in electrical engineering from University of Shiraz, Shiraz, Iran, in 2010, the M.S. degree in electrical engineering from the Amirkabir University of Technology (Tehran Polytechnic), Tehran, Iran, in 2013. He is currently working toward the Ph.D. degree with the Erik Jonsson School of Engineering and Computer Science, The University of Texas at Dallas, Richardson, TX, USA. He is a member of the Open Networking Advanced Research (OpNeAR) Lab at The University of Texas at Dallas. His research interests include SDN-enabled WDM networks, optical flow switching, optical networks simulation, multi-layer network planning, optimization, and orchestration.

Behzad Mirkhanzadeh received the B.S. degree in software engineering from Shiraz University, Shiraz, Iran, in 2013. He has been researching and working on programmable networks and SDN since 2014. He was employed by the IIS center of Sharif University of Technology as a Software/Network Engineer during 2014–2016 to develop an OSS/BSS system for a carrier-grade telecommunication company in Iran. He has been working with the OpNeAR Lab, University of Texas at Dallas as a Research Assistant since September 2016, while working toward the Ph.D. degree in telecommunications engineering. He has particular interests in multi-layer SDN, SDWAN, data center interconnections, cloud computing, and NFV.

Chencheng Shao, biography not available at the time of publication.

Miguel Razo, biography not available at the time of publication.

Marco Tacca, biography not available at the time of publication.

Alessio Ferrari, biography not available at the time of publication.

Mattia Cantono, biography not available at the time of publication.

Vittorio Curri, biography not available at the time of publication.

Giovanni Martinelli, biography not available at the time of publication.

Gabriele Maria Galimberti, biography not available at the time of publication.

Tiejun Xia, biography not available at the time of publication.

Glenn Wellbrock, biography not available at the time of publication.

Andrea Fumagalli, biography not available at the time of publication.